



Absence of Detectable Arsenate in DNA from Arsenate-Grown GFAJ-1 Cells
 Marshall Louis Reaves *et al.*
Science **337**, 470 (2012);
 DOI: 10.1126/science.1219861

This copy is for your personal, non-commercial use only.

If you wish to distribute this article to others, you can order high-quality copies for your colleagues, clients, or customers by [clicking here](#).

Permission to republish or repurpose articles or portions of articles can be obtained by following the guidelines [here](#).

The following resources related to this article are available online at www.sciencemag.org (this information is current as of August 14, 2012):

Updated information and services, including high-resolution figures, can be found in the online version of this article at:

<http://www.sciencemag.org/content/337/6093/470.full.html>

Supporting Online Material can be found at:

<http://www.sciencemag.org/content/suppl/2012/07/06/science.1219861.DC1.html>

A list of selected additional articles on the Science Web sites **related to this article** can be found at:

<http://www.sciencemag.org/content/337/6093/470.full.html#related>

This article **cites 11 articles**, 6 of which can be accessed free:

<http://www.sciencemag.org/content/337/6093/470.full.html#ref-list-1>

This article appears in the following **subject collections**:

Microbiology

<http://www.sciencemag.org/cgi/collection/microbio>

17. G. R. Willsky, M. H. Malamy, *J. Bacteriol.* **144**, 356 (1980).
 18. D. Cánovas, C. Durán, N. Rodríguez, R. Amils, V. de Lorenzo, *Environ. Microbiol.* **5**, 133 (2003).

Acknowledgments: We thank R. Oremland and J. S. Blum for providing strain GFAJ-1, P. Christen and F. Ryffel for technical and experimental assistance, as well as an anonymous

reviewer for valuable suggestions and comments on our manuscript. T.J.E. was supported through an ETH Fellowship.

Supplementary Materials
www.sciencemag.org/cgi/content/full/science.1218455/DC1
 Materials and Methods

Figs. S1 to S3
 Tables S1 to S8
 References

27 December 2011; accepted 1 June 2012
 Published online 8 July 2012;
[10.1126/science.1218455](https://doi.org/10.1126/science.1218455)

Absence of Detectable Arsenate in DNA from Arsenate-Grown GFAJ-1 Cells

Marshall Louis Reaves,^{1,2} Sunita Sinha,³ Joshua D. Rabinowitz,^{1,4}
 Leonid Kruglyak,^{1,5,6} Rosemary J. Redfield^{3*}

A strain of *Halomonas* bacteria, GFAJ-1, has been claimed to be able to use arsenate as a nutrient when phosphate is limiting and to specifically incorporate arsenic into its DNA in place of phosphorus. However, we have found that arsenate does not contribute to growth of GFAJ-1 when phosphate is limiting and that DNA purified from cells grown with limiting phosphate and abundant arsenate does not exhibit the spontaneous hydrolysis expected of arsenate ester bonds. Furthermore, mass spectrometry showed that this DNA contains only trace amounts of free arsenate and no detectable covalently bound arsenate.

Wolfe-Simon *et al.* isolated strain GFAJ-1 from the arsenic-rich sediments of California's Mono Lake by its ability to grow through multiple subculturing in artificial Mono Lake medium AML60 that lacked added phosphate but had high concentrations of arsenate (+As/-P condition) (1). Because GFAJ-1 grew in -P medium only when arsenate was provided, and because substantial amounts of arsenate were detected in subcellular fractions, growth was attributed to the use of arsenate in place of phosphate. However, the basal level of phosphate contaminating the -P medium was reported to be 3 to 4 μM (1), which previous studies of low-phosphate microbial communities suggest is sufficient to support moderate growth (2). GFAJ-1 grew well on medium supplemented with ample phosphate but no arsenate (1500 μM PO_4 , +P/-As condition), indicating that GFAJ-1 is not obligately arsenate-dependent.

Wolfe-Simon *et al.* (1) further inferred that arsenic was incorporated into the DNA backbone of GFAJ-1 in place of phosphorus, with an estimated 4% replacement of P by As based on the As:P ratio measured in agarose gel slices containing DNA samples. This finding was surprising because arsenate is predicted to reduce rapidly

to arsenite in physiological conditions (3, 4) and because arsenate esters in aqueous solution are known to be rapidly hydrolyzed (5). We have now tested this report by culturing GFAJ-1 cells supplied by the authors (1) and by analyzing highly purified DNA from phosphate-limited cells grown with and without arsenate.

Wolfe-Simon *et al.* reported that GFAJ-1 cells grew very slowly in AML60 medium (doubling time ~ 12 hours) and that, when phosphate was not added to the medium, cells failed to grow unless arsenate (40 mM) was provided (1). How-

ever, although we obtained strain GFAJ-1 from these authors, in our hands GFAJ-1 was unable to grow at all in AML60 medium containing the specified trace elements and vitamins, even with 1500 μM sodium phosphate added as specified in (1). We confirmed the strain's identity using reverse transcription-polymerase chain reaction and sequencing of 16S ribosomal RNA, with primers specified by Wolfe-Simon *et al.* (1); this gave a sequence identical to that reported for strain GFAJ-1. We then found that addition of small amounts of yeast extract, tryptone, or individual amino acids to basal AML60 medium allowed growth, with doubling times of 90 to 180 min. Medium with 1 mM glutamate added was therefore used for subsequent experiments (6).

With 1500 μM phosphate but no added arsenate (Wolfe-Simon *et al.*'s -As/+P condition), this medium produced $\sim 2 \times 10^8$ cells/ml, similar to the -As/+P yield obtained by Wolfe-Simon *et al.* (1). As expected, the growth yield depended on the level of phosphate supplementation (Fig. 1), with even unsupplemented medium allowing growth to $\sim 2 \times 10^6$ cells/ml. Because analysis by inductively coupled plasma-mass spectrometry (ICP-MS) showed that this medium contained only 0.5 μM contaminating phosphate, our supplementation with an additional 3.0 μM phosphate replicates Wolfe-Simon *et al.*'s "-P" culture condition. The growth analyses shown in Fig. 1 were performed in the absence of arsenate and showed

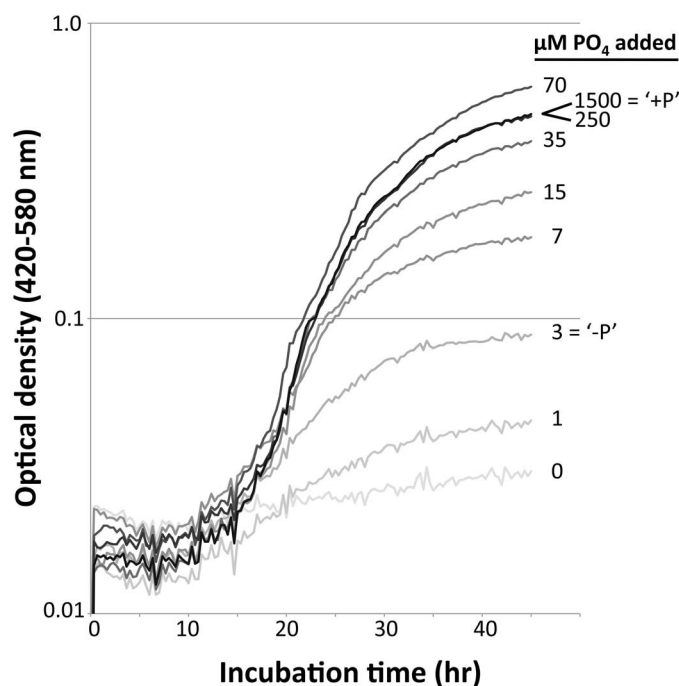


Fig. 1. Growth curves of GFAJ-1 in AML60 medium supplemented with different concentrations of phosphate. Each line is the mean of 10 replicate 300- μl cultures in wells of a Bioscreen C Growth Analyzer. The phosphate additions used to replicate the "-P" and "+P" conditions of (1) are indicated.

¹Lewis Sigler Institute for Integrative Genomics, Princeton University, Princeton, NJ 08544, USA. ²Department of Molecular Biology, Princeton University, Princeton, NJ 08544, USA. ³Department of Zoology, University of British Columbia, Vancouver, BC, Canada. ⁴Department of Chemistry, Princeton University, Princeton, NJ 08544, USA. ⁵Howard Hughes Medical Institute, Lewis-Sigler Institute for Integrative Genomics, Princeton University, Princeton, NJ 08544, USA. ⁶Department of Ecology and Evolutionary Biology, Princeton University, Princeton, NJ 08544, USA.

*To whom correspondence should be addressed. E-mail: redfield@zoology.ubc.ca

that GFAJ-1 does not require arsenate for growth in media with any level of phosphate.

The cause of the discrepancies between our growth results and those of Wolfe-Simon *et al.* is not clear. The arsenate dependence they observed may reflect the presence in their arsenate (purity and supplier unknown) of a contaminant that filled the same metabolic role as our glutamate supplement. Our +As and -As cultures grew to similar densities, and we did not observe any

cases in which +As cultures grew but -As cultures did not. The phosphate dependence we observed is also consistent with that expected from work on other species (2).

To investigate the possible incorporation of arsenate into the GFAJ-1 DNA backbone, we purified and analyzed DNA from GFAJ-1 cells grown in four differently supplemented versions of AML60 medium, matching those analyzed by Wolfe-Simon *et al.*—i.e., -As/-P: no arsenate,

3.5 μM phosphate; +As/-P: 40 mM arsenate, 3.5 μM phosphate; -As/+P: no arsenate, 1500 μM phosphate; +As/+P: 40 mM arsenate, 1500 μM phosphate. Initial purification of DNA consisted of two preliminary organic extractions, precipitation from 70% ethanol, digestion with ribonuclease and proteinase, two additional organic extractions, and a final ethanol precipitation (6). DNA was collected from 70% ethanol by spooling rather than centrifugation, because this reduces contamination with other substances insoluble in ethanol (7).

Wolfe-Simon *et al.* suggested that arsenate ester bonds in GFAJ-1 DNA might be protected from hydrolysis by intracellular proteins or compartmentalization of the DNA (8). We therefore tested whether purification exposed GFAJ-1 DNA to spontaneous hydrolysis. Gel analysis of DNA immediately after purification revealed fragments of >30 kb, whether cells were grown with limiting or abundant phosphate and with or without 40 mM arsenate (Fig. 2A). We also re-examined this DNA after 2 months of storage at 4°C. All preparations showed very similar-sized fragments of double-stranded DNA and of single-stranded DNA (Fig. 2, B and C), with no evidence of hydrolysis. *Haemophilus influenzae* DNA served as a control for gel migration, indicating that GFAJ-1 DNA is not associated with hydrolysis-protecting proteins or other macromolecules that might have persisted through the purification. Unless arsenate-ester bonds are intrinsically stable in DNA, our analysis estimates a minimum separation between arsenates in the DNA backbone of at least 25 kb, three orders of magnitude below that estimated by Wolfe-Simon *et al.*

Arsenate in bonds that were stable to spontaneous hydrolysis should be detectable as free arsenate, arsenate-containing mononucleotides, or arsenate-containing dinucleotides after enzymatic digestion of purified DNA. We therefore used liquid chromatography–mass spectrometry (LC-MS) to analyze GFAJ-1 DNA for arsenate after digestion with P1 and snake venom nucleases (6). Relevant molecular species were identified by negative-mode, full-scan, high-mass resolution LC-MS analysis (6). This method was used to analyze two independent replicate DNA preparations from cells grown in either +As/-P or -As/+P medium and fractions from CsCl gradient analyses of these DNAs.

The initial DNA preparations of +As/-P DNAs contained some free arsenate anion (H₂AsO₄⁻) (Table 1), at levels similar to those reported by Wolfe-Simon *et al.* (1). This arsenate was largely removed by three serial washes with distilled water; digested washed DNA contained arsenate at a level slightly higher than in the water blank (Fig. 3 and Table 1). Thus, we concluded that most of the arsenate we detected after preliminary DNA purification arose by contamination from the arsenate-rich (40 mM) growth medium.

Further analyses compared the nuclease-digested and washed fractions obtained from

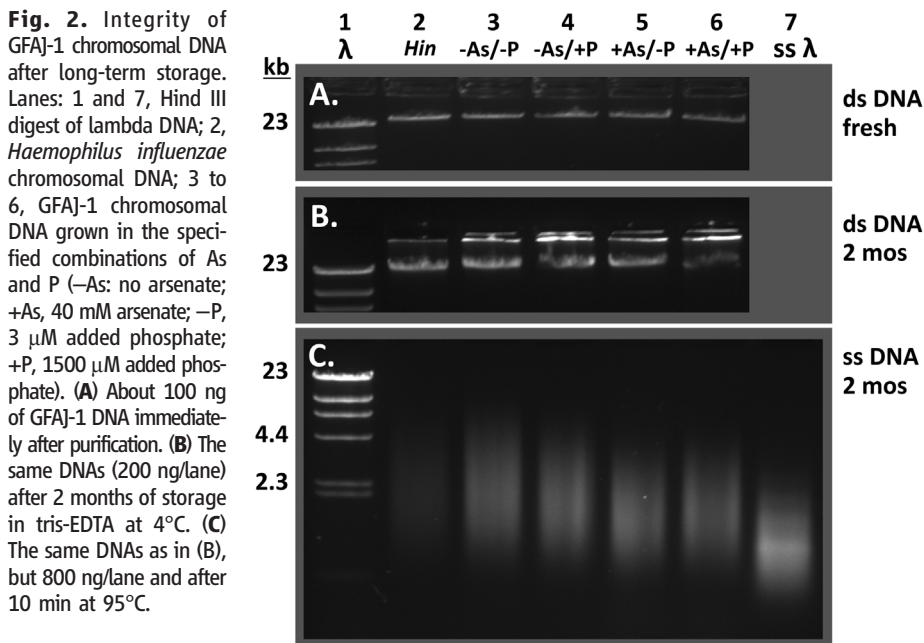


Table 1. DNA, arsenate, and nucleotide content of samples measured by absorbance at 260 nm and LC-MS. AU, absorbance units.

Sample	A ₂₆₀ (DNA) AU (μg)	Compound				
		Arsenate	dAMP	dAMA	dAMP-dAMP	dAMA-dAMP
		Peak area, ion counts				
Digested CsCl fractions: (increasing density)						
#1 (top)	0.03 (0)	0	0	154	0	0
#2	0.01 (0)	0	0	0	0	0
#3	0.02 (0)	226	0	0	0	0
#4	0.01 (0)	0	160	0	0	0
#5	0.01 (0)	0	0	0	0	0
#6	0.82 (4.5)	157	39,000	0	0	0
#7	1.12 (6.7)	373	52,000	0	0	0
#8 (bottom)	0.44 (1.9)	300	3,700	0	0	197
Water blank	0 (0)	329	0	0	0	0
-As/+P partial digest	(3.3)	515	0	0	21,000	210
+As/-P washed, digested DNA	(1.7)	2625	186,457	0	241	202
+As/-P whole DNA (1:10 dil.)	(1.7)	2794	562	0	781	0
+As/-P wash of gDNA (300 μl)	0 (0)	9545	182	207	0	221
Arsenate standards (molar)						
1.66 × 10 ⁻⁸		329				
1.66 × 10 ⁻⁷		1959				
1.66 × 10 ⁻⁵		59,925				
Expected if DNA As:P = 0.04	(6.7)	~122,000		>0		>0

CsCl isopycnic density gradient centrifugation of the DNAs (Fig. 3) (6). The arsenate detection limit for these measurements was $\sim 5 \times 10^{-8}$ M (table S1), a level that if present in the fractions with the most DNA would correspond to an As:P ratio of $<0.1\%$, 50-fold lower than the 4% ratio estimated by Wolfe-Simon *et al.* Although traces of arsenate (or a contaminant of mass similar to that of arsenate) were found in several fractions of the CsCl gradient, the arsenate peak did not exceed the limit of detection, and a similar-intensity signal at a mass-to-charge ratio (m/z) of arsenate was observed in the water blank. There was no evidence that the arsenate trace comigrated with the DNA. In contrast, normal phosphate-containing deoxynucleotides were observed in rough proportion to the abundance of DNA throughout the gradient for both the +As/-P and -As/+P cells (Fig. 4A and table S2).

Likewise, no arsenate-conjugated mono- or dinucleotides were detected by exact mass (Fig.

4, B and D). Although retention time and ionization efficiency could not be validated with standards for these molecules, their behavior, if the molecules were stable, would be expected to resemble that of their phosphorylated analogs sufficiently to allow detection. Finally, an enrichment of deoxynucleosides per nanogram of DNA obtained from GFAJ-1 grown in the +As/-P condition, relative to either -As/+P or -As/-P conditions, could indicate nicked DNA resulting from arsenate-ester hydrolysis. However, we did not detect any enrichment despite detecting deoxyadenosine, deoxyguanosine, deoxycytidine, and thymidine (fig. S1 and table S2). Thus, although we detected arsenate associated with GFAJ-1 DNA, we found no evidence for arsenate bound sufficiently tightly to resist washing with water or able to comigrate with the DNA in a CsCl gradient. Differences in DNA purity can readily explain the conflict of these results with Wolfe-Simon *et al.*'s claim that GFAJ-1 uses arsenate to replace scarce phosphate in its DNA.

Our LC-MS analyses rule out incorporation of arsenic in DNA at the $\sim 0.1\%$ level, and a much lower limit is suggested by our gel analysis of DNA integrity. Given the chemical similarity of arsenate to phosphate, it is likely that GFAJ-1 may sometimes assimilate arsenate into some small molecules in place of phosphate, such as sugar phosphates or nucleotides. Although the ability to tolerate or correct very-low-level incorporation of arsenic into DNA could contribute to the arsenate resistance of GFAJ-1, such low-level incorporation would not be a biologically functional substitute for phosphate, and thus would have no appreciable effect on the organism's requirements for phosphate.

From a broader perspective, GFAJ-1 cells growing in Mono Lake face the challenge of discriminating an essential salt (PO_4 , 400 μM) from a highly abundant but toxic chemical mimic (AsO_4 , 200 μM). Similar salt management challenges are encountered by many other microorganisms, such as those growing in environments

Fig. 3. LC-MS analysis of arsenate in purified and CsCl-fractionated DNA from arsenate-grown GFAJ-1 cells. Representative extracted ion chromatograms for arsenate [$m/z = 140.9174 \pm 3$ parts per million (ppm)] are shown as the chromatographic retention time (in minutes) plotted against intensity (in ion counts). Sample identity is indicated to the right, along the axis extending into the page. DNA from arsenate-grown GFAJ-1 cells (+As/-P undigested gDNA) was analyzed by LC-MS at a 1:10 dilution, as were the water wash (+As/-P wash of gDNA), the same DNA after washing and enzymatic digestion (+As/-P washed, digested DNA), and finally, fractions of the same DNA after a CsCl gradient purification and digestion (+As/-P CsCl fractions #1 to #8, with DNA concentrating in fractions #6, #7, and #8). Potassium arsenate standards (Std 1.7e-6 to 1.7e-8 [M]) and a water blank were also analyzed. One of four representative experiments is shown.

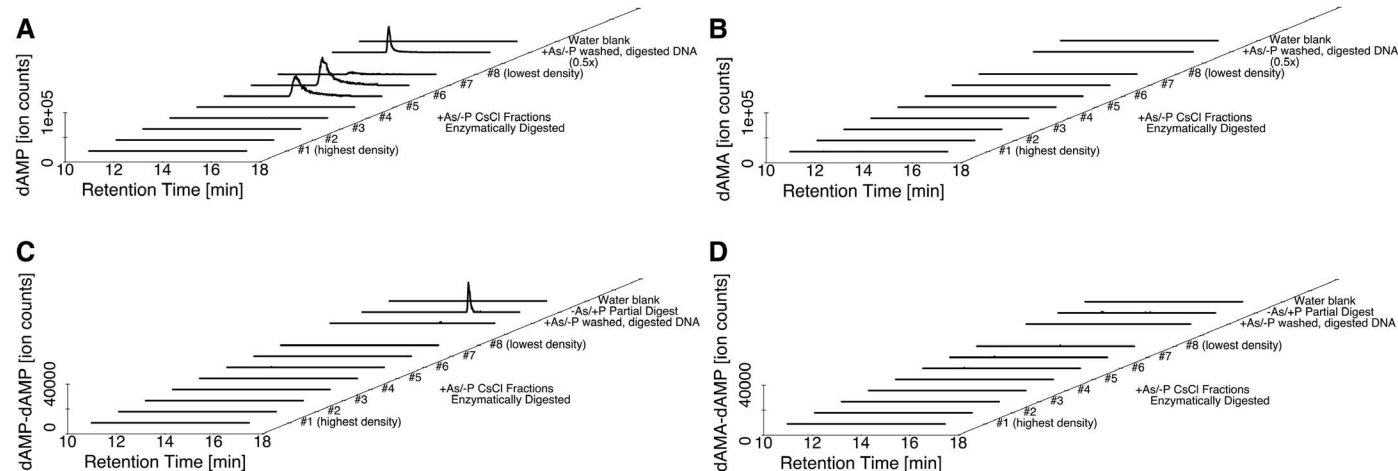
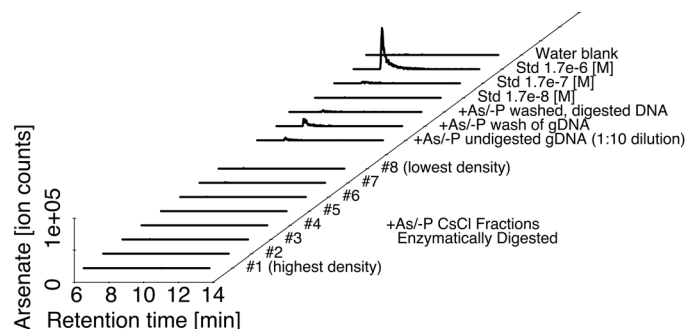


Fig. 4. LC-MS analysis of deoxynucleotides from purified and CsCl-fractionated DNA from arsenate-grown GFAJ-1 cells. Representative extracted ion chromatograms are shown as the chromatographic retention time (in minutes) plotted against intensity (in ion counts). One of four representative experiments is shown. (A and B) Extracted ion chromatograms for (A) deoxyadenosine-phosphate (dAMP; $m/z = 330.0609 \pm 5$ ppm) and (B) its arsenate analog deoxyadenosine-arsenate (dAMA; $m/z = 374.0087 \pm 5$ ppm). DNA from arsenate-grown GFAJ-1 cells (+As/-P washed, digested DNA) was washed, digested, and analyzed by LC-MS, as was the same DNA after a CsCl gradient purification and digestion (+As/-P CsCl fractions #1 to #8). To keep the peak

on scale, the signal for +As/-P washed, digested DNA has been multiplied by 0.5. This observed large peak matches the known retention time of dAMP. (C and D) Extracted ion chromatograms for (C) the dideoxynucleotide deoxyadenosine-phosphate (dAMP-dAMP; $m/z = 643.1185 \pm 5$ ppm) and (D) its mono-arsenate analog deoxyadenosine-arsenate-deoxyadenosine-phosphate (dAMA-dAMP; $m/z = 687.0663 \pm 5$ ppm). DNA from arsenate-grown GFAJ-1 cells (+As/-P washed, digested DNA) was washed, digested, and analyzed by LC-MS, as was the same DNA after a CsCl gradient purification and digestion (+As/-P CsCl fractions #1 to #8). Partially digested -As/+P DNA shows a large peak at the exact mass of dAMP-dAMP.

with scarce potassium and plentiful ammonia (9). Organisms typically adapt to such conditions not by incorporating the mimic in place of the essential salt but by enriching for the salt at multiple stages, from preferential membrane transport to the selectivity of metabolic enzymes. The end result is that the fundamental biopolymers conserved across all forms of life remain, in terms of chemical backbone, invariant (10–12).

References and Notes

1. F. Wolfe-Simon *et al.*, *Science* **332**, 1163 (2011).
2. J. B. Cotner, E. K. Hall, J. T. Scott, M. Haldal, *Front Microbiol* **1**, 132 (2010).
3. B. Schoepp-Cothenet *et al.*, *Science* **332**, 1149–j (2011).
4. E. Lebrun *et al.*, *Mol. Biol. Evol.* **20**, 686 (2003).

5. C. Baer, J. O. Edwards, P. H. Rieger, *Inorg. Chem.* **20**, 905 (1981).
6. Materials and methods are available as supplementary materials on *Science Online*.
7. O. T. Avery, C. M. Macleod, M. McCarty, *J. Exp. Med.* **79**, 137 (1944).
8. F. Wolfe-Simon *et al.*, *Science* **332**, 1149–j (2011).
9. D. C. Hess, W. Lu, J. D. Rabinowitz, D. Botstein, *PLoS Biol.* **4**, e351 (2006).
10. L. Wang *et al.*, *Proc. Natl. Acad. Sci. U.S.A.* **108**, 2963 (2011).
11. W. Lu *et al.*, *Anal. Chem.* **82**, 3212 (2010).
12. M. T. Zimmermann, A. Kloczkowski, R. L. Jernigan, *BMC Bioinformatics* **12**, 264 (2011).

Acknowledgments: M.L.R. is supported by a Graduate Research Fellowship from the National Science Foundation. J.D.R. is supported by the CAREER Award from the National Science Foundation. L.K. is an Investigator of the Howard

Hughes Medical Institute and a James S. McDonnell Foundation Centennial Fellow. R.J.R. thanks the Canadian Institutes of Health Research for funding and J. Blum and R. Oremland for providing strain GFAJ-1; M. Khoshnoodi for the trace-element mix; the Charles Thompson lab for use of their BioScreen Analyzer; and S. Silver and C. Rensing for helpful discussions. We also thank the ICP Laboratory in the Department of Geosciences at Princeton University for assistance with ICP-MS analysis.

Supplementary Materials

www.sciencemag.org/cgi/content/full/science.1219861/DC1
Materials and Methods
Fig. S1
Tables S1 and S2
References

31 January 2012; accepted 1 June 2012
Published online 8 July 2012;
10.1126/science.1219861

The Structure and Catalytic Cycle of a Sodium-Pumping Pyrophosphatase

Juho Kellosoalo,^{1,2*} Tommi Kajander,^{1*} Konstantin Kogan,¹ Kisun Pokharel,^{1,3} Adrian Goldman^{1†}

Membrane-integral pyrophosphatases (M-PPases) are crucial for the survival of plants, bacteria, and protozoan parasites. They couple pyrophosphate hydrolysis or synthesis to Na⁺ or H⁺ pumping. The 2.6-angstrom structure of *Thermotoga maritima* M-PPase in the resting state reveals a previously unknown solution for ion pumping. The hydrolytic center, 20 angstroms above the membrane, is coupled to the gate formed by the conserved Asp²⁴³, Glu²⁴⁶, and Lys⁷⁰⁷ by an unusual “coupling funnel” of six α helices. Comparison with our 4.0-angstrom resolution structure of the product complex suggests that helix 12 slides down upon substrate binding to open the gate by a simple binding-change mechanism. Below the gate, four helices form the exit channel. Superimposing helices 3 to 6, 9 to 12, and 13 to 16 suggests that M-PPases arose through gene triplication.

Found in plants, protozoans, bacteria, and archaea, membrane-integral pyrophosphatases (M-PPases) contain 14 to 17 transmembrane (TM) helices (1) and link pyrophosphate (PP_i) hydrolysis or synthesis to sodium or proton pumping (2). PPases are essential to drive anabolic reactions such as DNA synthesis to completion. In contrast to the soluble PPases, M-PPases recycle part of the free energy of PP_i hydrolysis to generate electrochemical potential across biological membranes. In plants, they are vital for maturation and enhance survival under abiotic stress conditions (drought, anoxia, cold) (3). They also are important for proliferation of disease causing protozoa (4).

Unlike the rotary F-type adenosine triphosphatases (F-ATPases), M-PPases are dimeric (5), and, unlike the P-type ATPases, there is no phosphorylated enzyme intermediate (6). M-PPases

can be divided into three functional classes: K⁺-independent proton pumps and K⁺-dependent sodium and proton pumps, both of which require potassium for maximal activity (2). The resting enzyme state is EMg₂, and two more metal ions bind with substrate, Mg₂PP_i (7).

We have solved the structure of the Na⁺-pumping M-PPase of *Thermotoga maritima* (TmPPase) in the resting state (TmPPase:Ca:Mg) at 2.6 Å resolution ($R_{\text{work}}/R_{\text{free}} = 20.5/24.5\%$) and with product bound (TmPPase:P_i:Mg₄) at 4.0 Å ($R_{\text{work}}/R_{\text{free}} = 29.5/36.5\%$) (tables S1 and S2, Fig. 1, and fig. S1). In addition, the tungstate derivative used to solve the structure corresponds to the TmPPase:M₂:P_i state (8), thus mapping out the catalytic cycle. TmPPase is a dimer of two very similar (rmsd/C α 0.58 Å) monomers, each with 16 TM helices (Fig. 1). The helices extend up to 25 Å from the membrane bilayer on the cytoplasmic side but end near the bilayer on the periplasmic side (Fig. 1 and fig. S2). The dimer interface comprises helices 10, 13, and 15 (fig. S2) and a short antiparallel β sheet in the sixth periplasmic loop between TM12 and 13. Although the protein is an obligate dimer, residue conservation (fig. S3) shows that the pump is located entirely within a single monomer. It had been suggested that TmPPase

was structurally similar to the F-ATPases (9), but a DALI search (10) shows that the only homologous structure is the recently published mung bean H⁺-pumping K⁺-dependent PPase (VrPPase) (11).

The unusual active site has four distinct regions: the hydrolytic center, some 20 Å above the membrane surface; a “coupling funnel”; the gate (closed in our structure) just below the membrane surface; and an exit channel for Na⁺ ions (Fig. 2A). The distance from the hydrolytic center to the gate is thus about 20 Å. Six helices, 5–6, 11–12, and 15–16 form the hydrolytic center and coupling funnel, whereas only helices 5, 6, 12, and 16 form the gate and channel, creating an internal “symmetry mismatch” (12) between the two regions. Conserved charged residues, many of which have been extensively mutated in M-PPases (fig. S4 and table S3) line the hydrolytic center, coupling funnel, and gate. Their positioning confirms that M-PPases arose by gene triplication (13). Helices 3 to 6, 9 to 12, and 13 to 16 of TmPPase, which carry all of the functional residues (Fig. 2), share a similar structural motif (Fig. 1) not found in other proteins except the VrPPase. The structural alignments align key conserved residues (fig. S2C) that cluster in the active site.

Our native 2.6 Å structure has one Ca²⁺ and one Mg²⁺ ion bound. The Ca²⁺ ion is coordinated by the conserved Asp⁶⁸⁸, Asp⁶⁹², and Asp⁶⁶⁰, which are positioned by Lys⁶⁶³, Lys⁶⁶⁴, and Lys⁶⁹⁵ (Fig. 2C and fig. S1), whereas the Mg²⁺ ion is coordinated by Asp²³² and Asp⁴⁶⁵ (fig. S1). The VrPPase structure, crystallized in the presence of Mg²⁺ and the competitive inhibitor imidodiphosphate (PNP) (11), contains two ions with about the same protein coordination (VrPPase M3 and M2) that are coordinated to the PNP inhibitor. We thus assign our Ca²⁺ as M1 (their M3) and our Mg²⁺ as M2 (their M2) because these are the two metal ions bound in the resting enzyme and because the Ca²⁺ is multivalently coordinated in both structures (11), unlike M2, which only binds Asp⁴⁶⁵⁽⁵⁰⁷⁾ in VrPPase (VrPPase numbers in parentheses). In addition, Gd³⁺, which inhibits TmPPase, binds at these two sites (fig. S5). The

¹Structural Biology and Biophysics Program, Institute of Biotechnology, Post Office Box 65, University of Helsinki, FIN-00014, Finland. ²Graduate School of Informational and Structural Biology, Finland. ³Department of Biochemistry and Food Chemistry, FIN-20014 University of Turku, Finland.

*These authors contributed equally to this work.

†To whom correspondence should be addressed. E-mail: adrian.goldman@helsinki.fi